

Synchronization and Localization in Ad-Hoc ICAS Networks Using a Two-Stage Kuramoto Method

Dominik Neudert-Schulz* , Thomas Dallmann* 

{first name}.{last name}@tu-ilmenau.de

*Radio Technologies for Automated and Connected Vehicles Research Group

Technische Universität Ilmenau

Ilmenau, Germany

Abstract—To enable Integrated Communications and Sensing (ICAS) in a peer-to-peer vehicular network, precise synchronization in frequency and phase among the communicating entities is required. In addition, self-driving cars need accurate position estimates of the surrounding vehicles. In this work, we propose a joint, distributed synchronization and localization scheme for a network of communicating entities. Our proposed scheme is mostly signal-agnostic and therefore can be applied to a wide range of possible ICAS signals. We also mitigate the effect of finite sampling frequencies, which otherwise would degrade the synchronization and localization performance severely.

Index Terms—synchronization, syntonization, localization, ICAS, Kuramoto, frequency, phase

I. INTRODUCTION

Vehicular networks are envisioned to be able to support Integrated Communications and Sensing (ICAS). That is, data transmission and radar applications shall be possible using the same signal. Such signals may be communication signals like OFDM (communication-centric ICAS) or dedicated radar signals like FMCW or pulse radar (radar-centric ICAS). Hence, there is a rich zoo of signals that might be considered for future ICAS applications.

In situations where there is no central coordinating unit, the communicating entities, from now on called *hosts*, need to cooperate on a peer-to-peer (P2P) basis. In order to allow for the most accurate radar applications, coherent signal processing is required. [1] For P2P scenarios, this means that hosts need to be synchronized exactly in both, frequency and phase. Moreover, precise position information may be required to support self-driving applications. However, especially in urban scenarios low-cost global navigation satellite systems (GNSS) receivers often fail to provide exact position estimates. [2], [3]

Phase and frequency synchronization is a long-standing problem. Consensus based algorithms as proposed in [4], [5], and [6] are able to solve this problem in a fully distributed manner. However, they either neglect the propagation delay completely or do not contribute to position estimation.

This work builds on the synchronization schemes proposed in [6] and [4]. The basis is the Kuramoto model [7], that is used to describe the convergence behavior of a large number of coupled oscillators. In [4], it has been shown that it is

This work has been funded by the German Research Agency (DFG) under the project JCRS CoMP under project number 504990291.

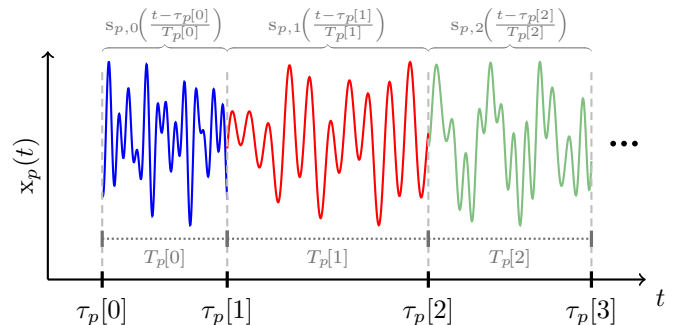


Fig. 1: Exemplary transmit signal $x_p(t)$ of some host p consisting of several base signals $s_{p,n}(t)$

possible to obtain frequency consensus in a network, that is designed to behave as a network of coupled oscillators. While the phase relation become stable, the phases themselves will not converge to a consensus. This problem is solved by the two-stage Kuramoto model described in [6]. However, both works ignore the effect of finite sampling frequencies and propagation delays in real-world applications. We close this gap making the two-stage Kuramoto method applicable to real-world scenarios. Since our proposed method also estimates the propagation delays between the hosts, we are able to perform mutual localization of all hosts.

This work is organized as follows: In Section II, we describe the signal model and a generalized phase definition. In Section III, we review the two-stage Kuramoto method and show how to acquire the required phase differences. Section IV outlines our proposed synchronization and localization algorithm. In Section V, we use simulations to validate our algorithm in different scenarios. Finally, Section VI concludes this work.

Notation: Throughout this work, vectors and matrices are denoted by bold lower-case and upper-case letters, respectively. A hat $\hat{\cdot}$ on top of a variable denotes the estimate of the corresponding variable. We will use T and $\|\cdot\|_F$ to denote the matrix transpose and the Frobenius norm, respectively.

II. SYSTEM MODEL

In this section, we will highlight the signal model and derive the phase difference definition used in the following sections.

A. Signal model

We consider a number of P simultaneously transmitting and receiving hosts. Each host transmits a signal $x_p(t) : \mathbb{R} \rightarrow \mathbb{C}$, where p is the index of the host. This signal is a concatenation of *base signals* $s_{p,n}(u) : \mathbb{R} \rightarrow \mathbb{C}$, with $n \in \mathbb{N}_0$. The actual form of the base signals $s_{p,n}(u)$ is not important as long as the following constraints are guaranteed:

- 1) A receiving host must be able to deduce the host which transmitted a base signal.
- 2) A receiving host must be able to determine the reception time of each transmitted base signal $s_{p,n}(u)$ with sufficient precision. This must hold true even if multiple hosts are transmitting simultaneously and even if the base signals overlap in time due to multipath propagation.
- 3) The base signals are causal ($s_{p,n}(u) = 0$ for $u < 0$) and have unit duration ($s_{p,n}(u) = 0$ for $u \geq 1$).

These constraints are often already fulfilled by practically used signals. Hence, the synchronization and localization algorithm presented later on is applicable to existing systems.

Let $T_{p,n}$ be the duration of the n -th base signal of host p and let $\tau_{\text{start},p}$ be the time of the first base signal transmitted by host p . The overall signal transmitted by host p is a concatenation of stretched or compressed base signals.

$$x_p(t) := \sum_{n=0}^{\infty} s_{p,n} \left(\frac{t - \tau_p[n]}{T_p[n]} \right) \quad (1)$$

$$\tau_p[n] := \tau_p[n-1] + T_p[n-1] = \tau_{\text{start},p} + \sum_{k=1}^{n-1} T_p[k] \quad (2)$$

$$\tau_p[0] := \tau_{\text{start},p}, \quad T_p[0] := T_{\text{start},p}$$

An exemplary depiction of such a signal $x_p(t)$ for some host p is shown in Fig. 1.

Even though a host may send a series of different base signals, we regard this model as a kind of quasi-periodic function where the signal duration $T_p[n]$ may change with every base signal.

On the receiving side, we consider a signal model, where some host q receives $K_{p,q}$ copies of the signal $x_p(t)$ transmitted by host p . These copies are attenuated by α_{p,q,k_p} and delayed by δ_{p,q,k_p} , where $k_p = 0 \dots K_{p,q} - 1$.

$$r_q(t) := \sum_{\substack{p=0 \\ p \neq q}}^{P-1} \sum_{k_p=0}^{K_{p,q}} \alpha_{p,q,k_p} x_p(t - \delta_{p,q,k_p}) \quad (3)$$

In this model, $k_p = 0$ corresponds to the line of sight (LOS) component. We presume that $\alpha_{p,q,0}$ is always sufficiently large such that for any pair of receiving host q and transmitting host p ($p \neq q$) the LOS component of the $n_{p,q}$ -th base signal from host p to host q can be detected and its reception time $t_{R,p,q}[n_{p,q}] := \tau_p[n_{p,q}] + \delta_{p,q,0}$ can be estimated.

As stated above, all hosts transmit their sequences of base signals. Every host starts to transmit at a different point in time. Moreover, each host has its own clock which is

usually not synchronized in time with the other hosts. Our goal is to synchronize all hosts ($p = 0 \dots P - 1$) so that their signal durations $T_p[n_p]$ and their base signal start times $\tau_p[n_p]$ each converge to a common value across all hosts as $n_p \rightarrow \infty$. Additionally, we will use the synchronization process to estimate the relative positions of hosts.

B. Phases and phase differences

We aim to synchronize the waveforms in signal duration and in pulse start times by utilizing the two-stage Kuramoto method. This method relies on a notion of a *phase*, for which we will now provide a definition tailored to our signal model.

A classical approach to define a phase involves the construction of an analytical signal $x_{\text{analytic},p} := x_p(t) + j\mathcal{H}\{x_p(t)\}$ using the Hilbert transform \mathcal{H} . In this case, the phase would be the angle in the complex plane $\varphi_{\text{analytic},p}(t) = \arg(x_{\text{analytic},p}(t))$. However, this only works well for narrow-band signals. Wideband signals could exhibit sudden spikes in $\varphi_{\text{analytic},p}(t)$. Therefore, we resort to an alternative phase definition.

Let $n_{T,q}(t)$ be the index of the base signal being transmitted by host q at time instant t . We define the *transmit phase* of $x_q(t)$ as follows.

$$\varphi_{T,q}(t) := 2\pi \left(n_{T,q}(t) + \frac{t - \tau_q[n_{T,q}(t)]}{T_q[n_{T,q}(t)]} \right) \quad (4)$$

The same idea is applied to the LOS signal $x_p(t - \delta_{p,q,0})$ from host p to host q . At some time instant t , let $n_{R,p,q}(t)$ be the index of the last base signal that host q received from host p . Then, we define the *receive phase* of $x_p(t - \delta_{p,q,0}(t))$ as:

$$\varphi_{R,p,q}(t) := 2\pi \left(n_{R,p,q}(t) + \frac{t - \delta_{p,q,0} - \tau_p[n_{R,p,q}(t)]}{T_p[n_{R,p,q}(t)]} \right) \quad (5)$$

The phase definitions presented in (4) and (5) are designed to have two main properties: First, the phase increases linearly from 0 to 2π within each base signal. Hence, the lengths of previous base signals do not influence the phase - only their number does. Second, besides the factor of 2π the slope of the phase within each base signals is an instantaneous frequency (i.e., inverse of signal duration).

The synchronization and localization approach presented in this work relies on the knowledge of a phase difference between the signal $x_q(t)$ sent by host q and the LOS signal $x_p(t - \delta_{p,q,0})$ sent by host p and received at host q . Note that pure synchronization would be possible with non-LOS components as well. Even a combination of multiple components may be possible. However, only the LOS allows us to estimate the distances between each host and therefore render localization possible.

Formally, the phase difference $\tilde{\psi}_{p,q}(t)$ between hosts q and p at time instant t could be defined as $\tilde{\psi}_{p,q}(t) := \varphi_{T,q}(t) - \varphi_{R,p,q}(t)$. Unfortunately, $\varphi_{R,p,q}(t)$ includes the signal duration $T_p[n_{R,p,q}(t)]$ of host p , which is not known at host q . One solution would be to use the previous signal duration of host p estimated by host q . Another approach presented in [4] simplifies the phase difference by assuming that host q 's signal

duration is roughly equal to host p 's signal duration leading to the approximation

$$\tilde{\psi}_{p,q}(t) \approx 2\pi \left(n_{\Delta,p,q}(t) + \frac{\tau_{\Delta,p,q}(t) + \delta_{p,q,0}}{T_q[n_{\text{T},q}(t)]} \right), \quad (6)$$

where

$$\begin{aligned} \tau_{\Delta,p,q}(t) &:= \tau_p[n_{\text{R},p,q}(t)] - \tau_q[n_{\text{T},q}(t)] \\ n_{\Delta,p,q}(t) &:= n_{\text{T},q}(t) - n_{\text{R},p,q}(t). \end{aligned}$$

In order to improve the accuracy of the phase difference estimate, a sampling factor N_s is introduced in [4], that includes multiple base signals into a single effective phase difference $\psi_{p,q}(t)$.

$$\psi_{p,q}(t) := \frac{2\pi}{N_s} \left(n_{\Delta,p,q}(t) + \frac{\tau_{\Delta,p,q}(t) + \delta_{p,q,0}}{T_q[n_{\text{T},q}(t)]} \right) \quad (7)$$

III. SYNCHRONIZATION AND LOCALIZATION

In this section, we review the two-stage Kuramoto method. After that, we show how we can estimate propagation delays based on the phase differences defined in (7).

A. The two-stage Kuramoto method

The two-stage Kuramoto method proposed in [6] can be used to synchronize hosts in frequency and phase. This method assumes that each host transmits at an instantaneous frequency $f_q(t)$, with $q = 0 \dots P - 1$, that can be decomposed into a base frequency $f_{\text{b},q}(t)$ and into an update term that depends on a phase differences $\Delta_{q,n_q}(t)$.

The first stage consists of a simple consensus filter which updates the base frequency.

$$\frac{df_{\text{b},q}(t)}{dt} = -\epsilon \sum_{\substack{p=0 \\ p \neq q}}^{N-1} (f_{\text{b},q}(t) - f_{\text{b},p}(t)) \quad (8)$$

The second stage describes the evolution of the instantaneous frequency $f_q(t)$. It resembles a first-order Kuramoto model with the intrinsic natural frequency being replaced by the base frequency $f_{\text{b},q}(t)$.

$$f_q(t) = f_{\text{b},q}(t) - \epsilon \sum_{\substack{p=0 \\ p \neq q}}^{P-1} \sin(\Delta_{q,n_q}(t)) \quad (9)$$

The authors of [6] could show that their two-stage Kuramoto method is capable of synchronizing the frequencies and the phases of a number of entities in a network. In the following sections, we will extend this method to add localization capabilities. Moreover, we will extend the first stage such that the method works also in the presence of sampling effects.

B. Estimating transmit times and propagation delays

The phase difference $\psi_{p,q}(t)$ defined in (7) includes the LOS propagation delay $\delta_{p,q,0}$. Hence, we cannot use $\psi_{p,q}(t)$ directly for frequency and phase synchronization.

To combat this, we decompose $\psi_{p,q}(t)$ into a phase difference $\psi_{\tau,p,q}(t)$ that only depends on the base signal start

times and into a phase difference $\psi_{\delta,p,q}(t)$ that includes the propagation delay:

$$\psi_{p,q}(t) := \psi_{\tau,p,q}(t) + \psi_{\delta,p,q}(t), \quad (10)$$

where

$$\psi_{\tau,p,q}(t) := \frac{2\pi}{N_s} \left(n_{\Delta,p,q}(t) + \frac{\tau_{\Delta,p,q}(t)}{T_q[n_{\text{T},q}(t)]} \right) \quad (11)$$

$$\psi_{\delta,p,q}(t) := 2\pi \frac{\delta_{p,q,0}}{N_s T_q[n_{\text{T},q}(t)]} \quad (12)$$

The joint synchronization and localization algorithm described in the following section requires knowledge of $\psi_{\tau,p,q}(t)$ and $\psi_{\delta,p,q}(t)$. Hence, we will now analyze, how the decomposition given in (10) can be computed. To this end, we rewrite (10) in terms of matrices as

$$\Psi = \Psi_{\tau} + \Psi_{\delta}, \quad (13)$$

where

$$\begin{aligned} [\Psi(t)]_{p,q} &:= \psi_{p,q}(t), & [\Psi_{\tau}(t)]_{p,q} &:= \psi_{\tau,p,q}(t), \\ [\Psi_{\delta}(t)]_{p,q} &:= \psi_{\delta,p,q}(t). \end{aligned}$$

For notational convenience, we will omit writing the dependency of these matrices on the time t .

Suppose that no base signal is lost during transmission. That is, all base signals transmitted by one host are eventually received by all other hosts. In this case, the number of transmitted base signals $n_{\text{T},p}(t)$ equals the number of received base signals $n_{\text{R},p,q}(t)$. It follows that $n_{\Delta,p,q}(t) = -n_{\Delta,q,p}(t)$. In the limit of perfectly synchronized pulse start times ($\tau_{\Delta,p,q}(t) = 0$), it holds that $\psi_{\tau,p,q}(t) = -\psi_{\tau,q,p}(t)$. Hence, Ψ_{τ} becomes a skew-symmetric matrix ($\Psi_{\tau} = -\Psi_{\tau}^T$).

Next, we exploit the fact that propagation delays are the same in both directions ($\delta_{p,q,0} = \delta_{q,p,0}$). In the limit of perfectly synchronized pulse durations ($T_p[n_{\text{T},p}(t)] = T_q[n_{\text{T},q}(t)]$) the phase differences $\psi_{\delta,p,q}(t)$ and $\psi_{\delta,q,p}(t)$ become equal. Hence, Ψ_{δ} becomes a symmetric matrix ($\Psi_{\delta} = \Psi_{\delta}^T$).

Finally, consider the case where both, the base signal start times and signal durations, are sufficiently synchronized, such that $\Psi_{\tau} \approx -\Psi_{\tau}^T$ and $\Psi_{\delta} \approx \Psi_{\delta}^T$. In this case, the decomposition given in (13) can be estimated as follows.

$$\Psi_{\tau} \approx \frac{1}{2} (\Psi - \Psi^T), \quad \Psi_{\delta} \approx \frac{1}{2} (\Psi + \Psi^T) \quad (14)$$

IV. PROPOSED ALGORITHM

In this section, we will explain our proposed synchronization process, that is executed on each host in order to continuously adapt the signal duration. To this end, we assume a fully connected network, where all hosts listen to the base signals transmitted by all other hosts.

A. Notation

In order to avoid an unnecessarily complex description of the proposed algorithm, we will resort to a simplified notation for the following subsections. Especially, we will omit the time dependency of various parameters, assuming the current point in time of reception or transmission, respectively. Moreover,

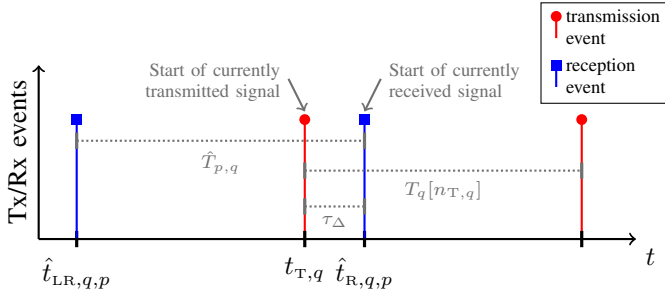


Fig. 2: Exemplary scenario as seen from host q : Host q receives base signals from host p and transmits its own base signals. Vertical lines indicate the point in time of transmission (red/circle) and reception (blue/square), respectively.

we will use the following quantities: Let $n_{T,q}$ denote the index of the base signal currently being transmitted by host q . This base signal started at time $t_{T,q}$ and has duration $T_q[n_{T,q}]$. Moreover, let $\hat{t}_{R,p,q}$ and $\hat{t}_{LR,p,q}$ denote the time – measured in host q 's time frame – at which the current base signal and the last base signal from host p arrived at host q , respectively. Host q 's index of the current base signal received from host p is $n_{R,p,q}$. Fig. 2 shows an exemplary scenario.

B. Distribution of estimated phase differences

During the synchronization process, each host p estimates a vector $\hat{\psi}_p$ of phase differences using (7). This vector is transmitted to all other hosts either in-band (modulated on the base signals) or via a separate communication channel (out-of-band). Note that, in order to save network resources, this vector may be transmitted less frequently than the base signals.

When a host q receives such a vector from host p , host q updates the p -th column of its estimated phase difference matrix $\hat{\Psi}_q$ (host q 's estimate of Ψ).

$$[\hat{\Psi}_q]_{:,p} \leftarrow \hat{\psi}_p \quad (15)$$

The q -th column of $\hat{\Psi}_q$ is updated upon reception of base signals as described in the next subsection.

C. Base signal reception

Upon reception of a base signal from some host p at time instant $\hat{t}_{R,p,q}$, host q estimates the phase difference between itself and host p . The estimated phase difference is stored in the matrix $\hat{\Psi}_q$. Based on (7), the phase difference is estimated as

$$[\hat{\Psi}_q]_{p,q} \leftarrow \frac{2\pi}{N_s} \left(n_\Delta + \frac{\tau_\Delta}{T_q[n_T]} \right), \quad (16)$$

where $\tau_\Delta := \hat{t}_{R,p,q} - t_{T,q}$ and $n_\Delta := n_{T,q} - n_{R,p,q}$.

In order to conduct the synchronization, host q needs to estimate the signal durations of all other hosts. To this end, every time host q receives a base signal from host p , it updates its estimate of host p 's signal duration $\hat{T}_{p,q}$ using the current reception time $\hat{t}_{R,p,q}$ and the previous reception time $\hat{t}_{LR,p,q}$.

$$\hat{T}_{p,q} \leftarrow \hat{t}_{R,p,q} - \hat{t}_{LR,p,q} \quad (17)$$

D. Localization

Once all columns of host q 's phase difference matrix $\hat{\Psi}_q$ are known, host q can estimate the phase matrix $\hat{\Psi}_{\delta,q}$ according to (14). After this, host q can utilize the propagation delays in $\hat{\Psi}_{\delta,q}$ to estimate relative positions of all other hosts using techniques like multidimensional scaling [8], [9].

E. Synchronization

The synchronization step estimates the duration $T_q[n_{T,q} + 1]$ of the next base signal to be transmitted by host q . This step requires that host q has estimated the signal durations $\hat{T}_{p,q}$ of all other hosts p as well as the q -th column of $\hat{\Psi}_{\tau,q}$. The matrix $\hat{\Psi}_{\tau,q}$ may either be computed via (14) or by subtracting $\hat{\Psi}_{\delta,q}$ from $\hat{\Psi}_q$.

First stage of Kuramoto method

This sub-step corresponds to the first stage of the two-stage Kuramoto method presented in [6] with an additional penalty term to prevent drift of the signal durations.

In this step, host q computes a base frequency $f_{b,q}$ using its estimated signal durations $\hat{T}_{p,q}$, where $\hat{T}_{q,q}$ shall be set to host q 's own current signal duration.

$$f_{b,q} \leftarrow \frac{1}{P} \sum_{p=0}^{P-1} \hat{T}_{p,q}^{-1} - \alpha_a \Delta_{a,q} t \quad (18)$$

The quantity $\Delta_{a,q}$ is a penalty that comes into play if the signal durations of all hosts jointly drift away. For this, host q has to choose an anchor frequency $f_{a,q}$.

$$\Delta_{a,q} \leftarrow \frac{1}{P} \sum_{p=0}^{P-1} \hat{T}_{p,q}^{-1} - f_{a,q} \quad (19)$$

The anchor frequency $f_{a,q}$ is assumed to be constant over the synchronization period. In this work, we chose $f_{a,q}$ to be the average over the initial signal durations $\hat{T}_{\text{start},p,q}$, where $\hat{T}_{\text{start},p,q}$ is host q 's estimate of the true initial pulse duration $T_{\text{start},p}$.

$$f_{a,q} := \frac{1}{P} \sum_{p=0}^{P-1} \hat{T}_{\text{start},p,q}^{-1} \quad (20)$$

The factor α_a should be a small positive value close to zero.

Second stage of Kuramoto method

The first stage of the Kuramoto method achieves synchronization of the signal durations $T_q[n]$. In order to synchronize the base signal start times $\tau_q[n]$ we use the second stage of the two-stage Kuramoto method, which defines the signal duration $T_q[n_{T,q} + 1]$ used for the next base signal.

$$T_q[n_{T,q} + 1] \leftarrow \left(f_{b,q} - \frac{K}{P} \sum_{p=0}^{P-1} \sin \left([\hat{\Psi}_{\tau,q}]_{p,q} \right) \right)^{-1} \quad (21)$$

Here, the main diagonal of $\hat{\Psi}_{\tau,q}$ is defined to be zero.

V. SIMULATION

In this section, we will validate our proposed synchronization and localization scheme by means of simulations.

A. Simulation setup

We simulated four hosts. Their initial signal duration, initial transmit start times, and their positions are listed in Table I. Each host transmits a base signal and performs the proposed algorithm. The simulation assumes ideal conditions without noise or interference.

host	$T_{\text{start},\cdot} / f_{\text{start},\cdot}$	$\tau_{\text{start},\cdot}$	position
0	142.86 ns / 7.00 MHz	64.29 ns	$[0 \text{ m}, 0 \text{ m}, 0 \text{ m}]^T$
1	125.00 ns / 8.00 MHz	6.25 ns	$[30 \text{ m}, 10 \text{ m}, 0 \text{ m}]^T$
2	136.99 ns / 7.30 MHz	22.60 ns	$[10 \text{ m}, -30 \text{ m}, -10 \text{ m}]^T$
3	131.58 ns / 7.60 MHz	32.89 ns	$[20 \text{ m}, -25 \text{ m}, 20 \text{ m}]^T$

TABLE I: Host parameters

To show the effect of the sampling on the proposed synchronization approach, we conducted simulations with three different scenarios. In scenario A, we assumed perfect sampling without any error (i.e., infinite sampling frequency). In scenario B, we assumed a finite sampling frequency but no drift compensation ($\alpha_a = 0$). In scenario C, we also assumed a finite sampling frequency but this time with applied drift compensation. Table II summarizes the different scenarios and their parameters.

scenario	f_s	α_a	comment
A	∞ Hz	0	no sampling error
B	800.00 MHz	0	no drift compensation
C	800.00 MHz	0.05	with drift compensation

TABLE II: Simulated scenarios

B. Performance metrics

For each simulation setup, we will analyze the synchronization in phase and frequency as well as the localization.

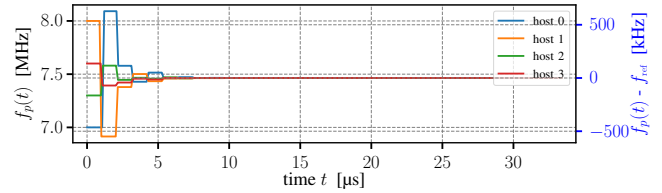
The first plot (a) of each scenario depicts the evolution of the instantaneous frequency $f_p(t) := 1/T_p[n_{\text{T},p}(t)]$ of each host p over time. The left axis shows the actual instantaneous frequency, while the right axis shows the difference to a reference frequency f_{ref} . The reference frequency is provided below each plot (a).

The phase synchronization is measured via the transmit start times $\tau_p[n_{\text{T},p}(t)]$ of each host. In plot (b) of each scenario, we depict the error function $\text{err}_{\text{start},p}(t)$.

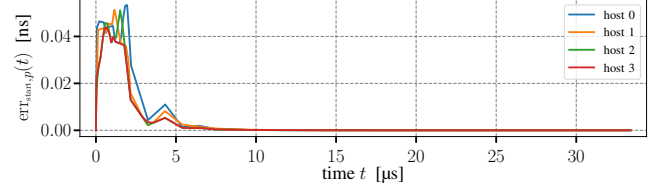
$$\text{err}_{\text{start},p}(t) := \frac{1}{P-1} \sum_{\substack{q=0 \\ q \neq p}}^{P-1} |\tau_p[n_{\text{T},p}(t)] - \tau_q[n_{\text{closest},q}(t)]| \quad (22)$$

$$n_{\text{closest},q}(t) := \arg \min_n |\tau_q[n] - \tau_q[n]| \quad (23)$$

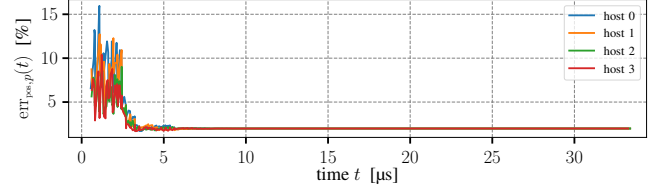
For each transmit time $\tau_p[n_{\text{T},p}(t)]$ of some host p , $\text{err}_{\text{start},p}(t)$ looks for the nearest transmit time of all other hosts and computes the mean absolute difference. This value should go to zero as the hosts synchronize their transmit times.



(a) Instantaneous frequency $f_p(t)$ ($f_{\text{ref}} = 7464.103$ kHz)



(b) Mean absolute differences of base signal start times



(c) Relative position error

Fig. 3: Scenario A: Simulation without sampling error

Finally, we analyze the localization error by looking at the relative position error $\text{err}_{\text{pos},p}(t)$.

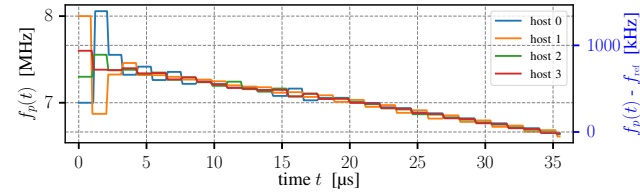
$$\text{err}_{\text{pos},p}(t) := \frac{\|\mathbf{X} - \mathbf{C}(\mathbf{A}, \mathbf{B}) \hat{\mathbf{X}}_p(t)\|_{\text{F}}}{\|\mathbf{X}\|_{\text{F}}} \quad (24)$$

Here, \mathbf{X} is a matrix whose columns contain the true host positions and $\hat{\mathbf{X}}_p(t)$ is host p 's estimate of the position matrix at time t . The estimated position matrices $\hat{\mathbf{X}}_p(t)$ contain only relative positions. Therefore, we pre-multiply $\hat{\mathbf{X}}_p(t)$ by a rotation matrix $\mathbf{C}(\mathbf{A}, \mathbf{B})$ computed via Procrustes analysis such that $\|\mathbf{A} - \mathbf{C}(\mathbf{A}, \mathbf{B}) \mathbf{B}\|_{\text{F}}$ is minimized (cf. [10]).

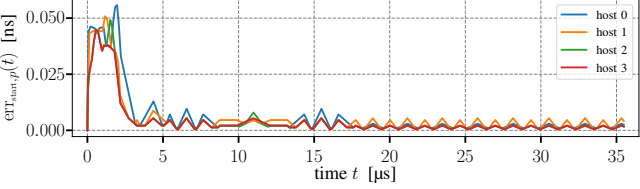
C. Results

Scenario A (Fig. 3) shows the results for the ideal case without sampling error. The instantaneous frequencies (Fig. 3a) and the transmit times (Fig. 3b) quickly converge to a common and constant value. Likewise, the localization error (Fig. 3c) tends to zero in the same amount of time.

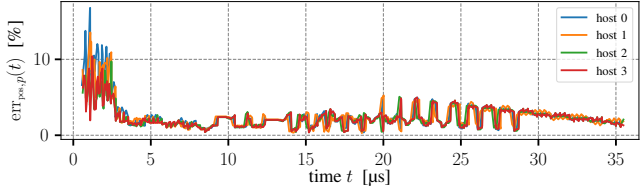
Fig. 4 depicts the results for scenario B with finite sampling frequency but without drift compensation. Here, the instantaneous frequencies (Fig. 4a) get closer to each other as well, though not as close as in the ideal case (scenario A). The main problem is that a joint drift is induced. As for the start times (Fig. 4b), these get closer to each other as well, with some oscillation remaining. As it can be seen on Fig. 4c, the position estimation is unstable under these conditions. Note from Table II that we used a sampling frequency which is roughly 100 times the initial base signal frequency. Even that



(a) Instantaneous frequency $f_p(t)$ ($f_{\text{ref}} = 6662.443$ kHz)



(b) Mean absolute differences of base signal start times



(c) Relative position error

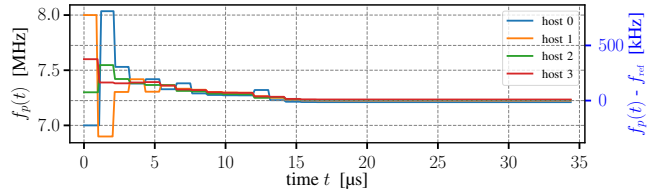
Fig. 4: Scenario B: Simulation with sampling error and without drift compensation

did not help to mitigate the negative effects of the induced sampling error.

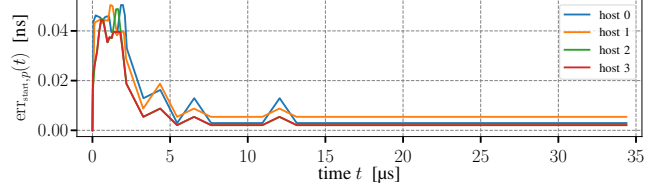
Finally, scenario C with finite sampling frequency and drift compensation is shown in Fig. 5. Here we used only a tiny amount of drift compensation as it can be seen Table II. Still, this small amount was sufficient to combat the frequency drift and to significantly improve the overall synchronization performance. The instantaneous frequencies (Fig. 5a) converge to a common and constant value again, similar to scenario A though not with the same remaining difference. Similar results are visible for the transmit times (Fig. 5b). The resulting start times are not as close as in scenario A, but significantly better compared to scenario B. The improved synchronization affects the localization accuracy (Fig. 5c). Here, the relative error does not approach zero as in scenario A, but the position estimates have become stable and much more reliable compared to scenario B.

VI. CONCLUSION

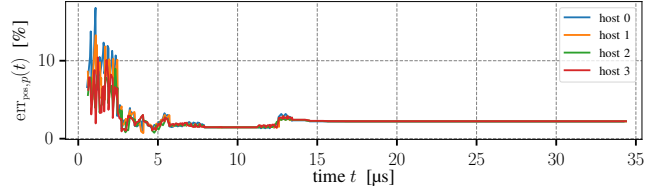
In this work, we extended the two-stage Kuramoto method for the synchronization of hosts in a wireless network to also support localization capabilities. We could show that the two-stage Kuramoto method is indeed capable of providing enough information to jointly localize the hosts. However, we demonstrated that real-world effects like sampling can significantly deteriorate the performance of both, the synchronization and the localization. To this end, we proposed a simple mechanism to mitigate the negative effects of finite sampling frequencies.



(a) Instantaneous frequency $f_p(t)$ ($f_{\text{ref}} = 7224.767$ kHz)



(b) Mean absolute differences of base signal start times



(c) Relative position error

Fig. 5: Scenario C: Simulation with sampling error and drift compensation

The mitigation improved the frequency and phase synchronization significantly and rendered the localization much more reliable.

REFERENCES

- [1] A. Elgamal, P. Knott, T. Dallmann, and S. Semper, "Multi-bistatic coordinated multipoint jcas: Exploring the synchronization requirements," in *2025 IEEE 5th International Symposium on Joint Communications & Sensing (JC&S)*, 2025, pp. 1–6.
- [2] P. D. Groves and M. Adjrad, "Performance assessment of 3d-mapping-aided gnss part 1: Algorithms, user equipment, and review," *NAVIGATION*, vol. 66, no. 2, pp. 341–362, 2019.
- [3] M. Adjrad, P. D. Groves, J. C. Quick, and C. Ellul, "Performance assessment of 3d-mapping-aided gnss part 2: Environment and mapping," *NAVIGATION*, vol. 66, no. 2, pp. 363–383, 2019.
- [4] T. Dallmann, "Sampling criteria for mutual over-the-air synchronisation of radar sensors," *Electronics Letters*, vol. 57, no. 18, pp. 702–704, 2021.
- [5] A. Bathelt, "An approach to consensus-based time synchronization based on dynamic consensus," *IEEE Control Systems Letters*, vol. 7, pp. 3319–3324, 2023.
- [6] A. Bathelt, V. Herath, and T. Dallmann, "An extended kuramoto model for frequency and phase synchronization in delay-free networks with finite number of agents," 2024. [Online]. Available: <https://arxiv.org/abs/2403.13440>
- [7] Y. Kuramoto, "Self-entrainment of a population of coupled non-linear oscillators," in *International Symposium on Mathematical Problems in Theoretical Physics*. Berlin, Heidelberg: Springer Berlin Heidelberg, 1975, pp. 420–422.
- [8] M. W. Richardson, "Multidimensional psychophysics," *Psychological Bulletin*, no. 35, pp. 659–660, 1938.
- [9] W. S. Torgerson, "Multidimensional scaling: I. theory and method," *Psychometrika*, vol. 17, no. 4, 1952.
- [10] P. H. Schönemann, "A generalized solution of the orthogonal procrustes problem," *Psychometrika*, vol. 31, no. 1, 1966.